INDUSTRIAL ENGINEERING

PETROLUEM ENGINEERIN

Journal of Engg. Research **Vol. 2 - (1) March 2014** pp. 1-31

ورقة مستضافة
استخدام وحدات التحكم الغير خطية لتزامن الأ نظمة المفرطة "الهايبركياتك"

***محمد الزريبي و ** نجيب السماوي**

* قسم الهندسة الكهربائية

** قسم الرياضيات، جامعة الكويت، ص ب 5969، الصفاة، 13060، الكويت

خلاصة

تناقش هذه الورقة تصميم وحدات التحكم الغير خطية لتزامن نظم "الهايبركياتك" الفوضى المفرطة. تستعمل قاعدة التغذية الاسترجاعية الخطية (FLC) وقاعدة التحكم الانزلاقي (SMC) لمزامنة نظامي لو (Lü) المتطابقين للفوضى المفرطة أحدهما أساسي والآخر ثانوي. نثبت أن الفرق بين متغيرات النظامين الأساسي والثانوي تئول إلى الصفر. كل النتائج المقدمة أثبتت تحليلياً وعددياً وقد تم عرض نتائج المحاكاة لتوضيح وتعزيز قدرة وحدة التحكم. وبالإضافة إلى ذلك، تم تطبيق قاعدة التحكم المقترحة في مجال الاتصالات المؤمّنة حيث تم تقديم نتائج المحاكاة الحاسوبية لإظهار كفاءة قاعدة التحكم المقترحة.

Invited paper

Synchronization of hyperchaotic systems using nonlinear controllers

MOHAMED ZRIBI* AND NEJIB SMAOUI**

**Department of Electrical Engineering,*
***Department of Mathematics,*
Kuwait University, P.O. Box 5969, Safat, 13060, Kuwait

ABSTRACT

This paper deals with the design of nonlinear controllers for the synchronization of two hyperchaotic systems. The feedback linearization control (FLC) technique as well as the sliding mode control (SMC) technique are used to synchronize two identical hyperchaotic Lü systems. We prove that the errors between the states of the master system and the states of the slave system converge to zero asymptotically. Simulations results are presented to validate the developed theory; these results indicate that the proposed control schemes work very well. In addition, the proposed synchronization schemes are applied to the secure communication field; the simulation results indicate that the proposed schemes are effective.

Keywords: Hyperchaotic systems; Synchronization; Feedback linearization control; Sliding mode control; Secure communication.

INTRODUCTION

The discovery of the Lorenz attractor (Lorenz, 1963) attracted many scientists and engineers to work on the theory and applications of chaos. For example, chaos has been used in optical communications (Argyris & Syvridis, 2010) in messages encryption (Babtista, 1998; Zribi, *et al.*, 2010; Smaoui, *et al.*, 2011) in image encryption, (Yau, *et al.*, 2012) in digital watermarking (Zhu & Sun 2012), in chaotic lasers (Uchida, 2012), in controlling motors (Zribi, *et al.*, 2009), and to monitor cardiac activity (Brandt & G. Chen, 1997). Pecora and Caroll (Pecora & Caroll, 1990) were the first to report that two identical chaotic systems can be synchronized. Synchronizing two chaotic systems means forcing these systems, through the use of controllers, to work in synchrony even though they start from two different initial conditions. The use of controllers forces the dynamics behavior of the slave system to be identical to the behavior of the master system after some transient time. It should be mentioned that the synchronization of chaotic systems has been studied extensively in the literature.

Hyperchaotic systems are known to be systems which are chaotic and possess more than one positive Lyapunov exponent. The most known hyperchaotic systems are the hyperchaotic Rossler system (Rossler, 1979; Chen, *et al.*, 2004; Hsieh, *et al.*, 1999; Jang, *et al.*, 2002), the hyperchaotic Chua circuit (Matsumoto, *et al.*, 1986; Kapitaniak, *et al.*, 1994; Itoh & Chua, 2002; Thamilmaran, *et al.*, 2004), the hyperchaotic Chen system (Chen, *et al.*, 2007; Smaoui, *et al.*, 2011; Yan, 2005) and the hyperchaotic Lü system (Chen, *et al.*, 2006; Gao & Lu, 2007; Jia, *et al.*, 2007; Yassen, 2008). The control and synchronization of hyperchaotic systems is a very active area of research as evident from the works of (Elabbasy, *et al.*, 2006; Feng, *et al.*, 2005; Gao, *et al.*, 2007; Grassi & Mascolo, 1999; Grassi & Miller, 2002; Hu, *et al.*, 2008; Huang, 2008; Jia, 2007; Jia, *et al.*, 2013; Li, *et al.*, 2005; Park, 2005; Rafikov & Balthazar, 2008; Sheikhan, *et al.*, 2013; Tao & Liu, 2007; Wang & Liu, 2007; Wu, *et al.*, 2008; Zhang, *et al.*, 2008; Zheng, *et al.*, 2010; Zhu, 2010) and the references therein.

In this paper, we investigate the synchronization of two hyperchaotic Lü systems using feedback linearization controllers and sliding mode controllers. The proposed techniques are successfully used for secure communication purposes.

The paper is organized as follows. A description of the hyperchaotic Lü system is presented in section 2. Section 3 and section 4 cover the design of a feedback linearization controller and a sliding mode controller for the synchronization of the hyperchaotic systems when the number of inputs to the slave system is three; simulation results are presented when these controllers are

used. Section 5 and section 6 present the design of a feedback linearization controller and a sliding mode controller when the number of inputs to the slave system is two; the developed theory is validated through simulations. Section 7 details the application of the proposed controllers for secure communication purposes. Finally some concluding remarks are given in section 8.

THE HYPERCHAOTIC LÜ SYSTEM

The dynamic model of the hyperchaotic *Lü* system is such that:

$$\begin{cases} \dot{x}(t) = a(y(t) - x(t)) + w(t) \\ \dot{y}(t) = -x(t)z(t) + cy(t) \\ \dot{z}(t) = x(t)y(t) - bz(t) \\ \dot{w}(t) = x(t)z(t) + rw(t) \end{cases} \tag{1}$$

where $x(t)$, $y(t)$, $z(t)$, $w(t)$ represent the state variables of the system; the parameters a, b, c and $> r$ are real constants. This system exhibits hyperchaotic behavior when $a = 36$, $b = 3$, $c = 20$ and $-0.35 < r \leq 1.3$. To illustrate this fact, the hyperchaotic *Lü* system is simulated with $r = 1$. The simulation results depicted in Figure 1 show the chaotic behavior of the system.

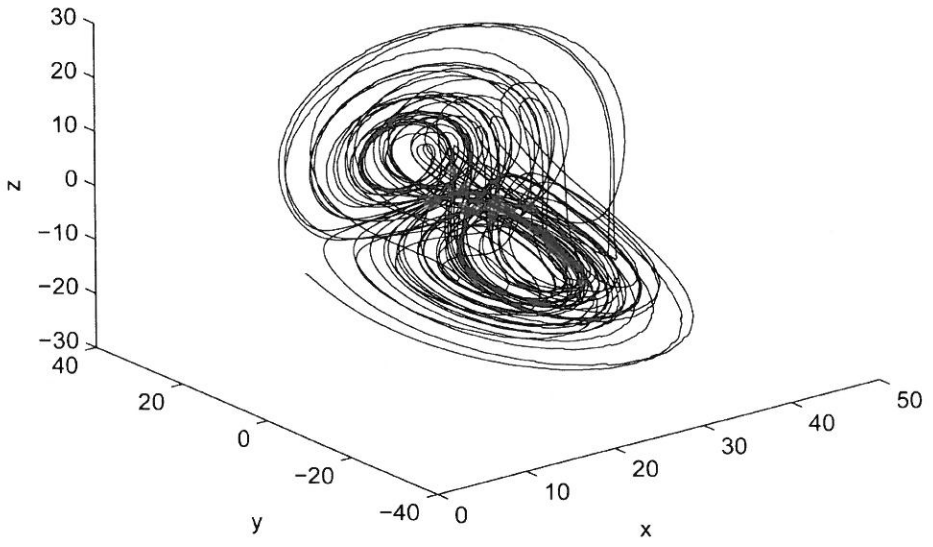

Fig. 1. The 3D phase plot of the the states of the hyperchaotic Lü system when $r = 1$

In this paper, we will study the synchronization problem of two identical

hyperchaotic Lü systems. Therefore, we need to define a master hyperchaotic L*ü* system and a slave hyperchaotic Lü system.

The model of the master hyperchaotic Lü system is as follows:

$$\begin{cases} \dot{x}_m(t) = a(y_m(t) - x_m(t)) + w_m(t) \\ \dot{y}_m(t) = -x_m(t)z_m(t) + cy_m(t) \\ \dot{z}_m(t) = x_m(t)y_m(t) - bz_m(t) \\ \dot{w}_m(t) = x_m(t)z_m(t) + rw_m(t) \end{cases} \tag{2}$$

The model of the slave hyperchaotic Lü system is defined as follows:

$$\begin{cases} \dot{x}_s(t) = a(y_s(t) - x_s(t)) + w_s(t) \\ \dot{y}_s(t) = -x_s(t)z_s(t) + cy_s(t) + u_1(t) \\ \dot{z}_s(t) = x_s(t)y_s(t) - bz_s(t) + u_3(t) \\ \dot{w}_s(t) = x_s(t)z_s(t) + rw_s(t) + u_2(t) \end{cases} \tag{3}$$

Note that the last three ordinary differential equations (odes) of the slave system given by equation (3) contain the $u_1(t)$, $u_2(t)$ and $u_3(t)$ terms. These terms represent the controllers of the system. These controllers will be designed such that the master system and the slave system are synchronized after starting from different initial conditions.

Define the errors between the states of the master system and the states of the slave system such that: $e_1(t) = x_s(t) - x_m(t)$, $e_2(t) = y_s(t) - y_m(t)$, $e_3(t) = z_s(t) - z_m(t)$ and $e_4(t) = w_s(t) - w_m(t)$. Also, let the error vector $e(t)$ be such that $e(t) = [e_1(t) \quad e_2(t) \quad e_3(t) \quad e_4(t)]^T$.

Using equations (2)-(3), the dynamic model of the errors between the slave and the master systems can be written as follows:

$$\begin{cases} \dot{e}_1(t) = a(e_2(t) - e_1(t)) + e_4(t) \\ \dot{e}_2(t) = -x_s(t)e_3(t) - z_m(t)e_1(t) + ce_2(t) + u_1(t) \\ \dot{e}_3(t) = x_s(t)e_2(t) + y_m(t)e_1(t) - be_3(t) + u_3(t) \\ \dot{e}_4(t) = x_s(t)e_3(t) + z_m(t)e_1(t) + re_4(t) + u_2(t) \end{cases} \tag{4}$$

The objective of the paper is to synchronize the master and the slave hyperchaotic Lü systems. Therefore, we will use nonlinear controllers to force

the errors $e_1(t)$, $e_2(t)$, $e_3(t)$ and $e_4(t)$ to converge to 0 as t tends to infinity. We propose to synchronize these systems using feedback linearization controllers and sliding mode controllers.

We will consider two cases. The first case is when the slave system has three control inputs; this case will be studied in sections 3 and 4. Then, we will consider the case when the slave system has two control inputs; this case will be analyzed in sections 5 and 6.

A FEEDBACK LINEARIZATION CONTROLLER WHEN THE SLAVE SYSTEM HAS 3 INPUTS

Design of the Controller

Let γ_1, γ_2 and γ_3 be positive scalars.

Theorem 1: The feedback linearization control laws:

$$\begin{aligned} u_1(t) &= -ae_1(t) + z_m(t)e_1(t) - ce_2(t) - \gamma_1 e_2(t) \\ u_2(t) &= -e_1(t) - x_s(t)e_3(t) - z_m(t)e_1(t) - re_4(t) - \gamma_2 e_4(t) \\ u_3(t) &= -y_m(t)e_1(t) - \gamma_3 e_3(t) \end{aligned} \tag{5}$$

when applied to the error system (4) guarantee the asymptotic convergence of the errors $e_i(t)$ $(i = 1, ..., 4)$ to zero as t tends to infinity.

Proof:

Let the Lyapunov function candidate $V(e)$ be such that:

$$V(e) = \frac{1}{2}e_1^2(t) + \frac{1}{2}e_2^2(t) + \frac{1}{2}e_3^2(t) + \frac{1}{2}e_4^2(t) \tag{6}$$

Note that the Lyapunov function candidate is positive definite as $V(e) = 0$ when $e(t) = 0$ and $V(e) > 0$ for $e(t) \neq 0$.

Using equations (4) and (5), the derivative of $V(e)$ with respect to time is such:

$$\begin{aligned} \dot{V}(e) &= e_1(t)(ae_2(t) - ae_1(t) + e_4(t)) + e_2(t)(-x_s(t)e_3(t) - z_m(t)e_1(t) + ce_2(t) + u_1(t)) \\ &\quad + e_3(t)(x_s(t)e_2(t) + y_m(t)e_1(t) - be_3(t) + u_3(t)) + e_4(t)(x_s(t)e_3(t) + z_m(t)e_1(t) + re_4(t) + u_2(t)) \\ &= -ae_1(t)^2 - be_3(t)^2 + e_2(t)(ae_1(t) - z_m(t)e_1(t) + ce_2(t) + u_1(t)) \\ &\quad + e_3(t)(y_m(t)e_1(t) + u_3(t)) + e_4(t)(e_1(t) + x_s(t)e_3(t) + z_m(t)e_1(t) + re_4(t) + u_2(t)) \\ &= -ae_1^2(t) - \gamma_1 e_2^2(t) - (b + \gamma_3)e_3^2(t) - \gamma_2 e_4^2(t) \end{aligned} \tag{7}$$

Since a, b, γ_1, γ_2, γ_3 are positive scalars, it can be concluded that $\dot{V}(e) = 0$ when $e(t) = 0$ and $\dot{V}(e) < 0$ for $e(t) \neq 0$. Hence, $V(e)$ is a positive definite function, $\dot{V}(e)$ is a negative definite function and $V(e)$ is radially unbounded. Therefore, the errors $e_1(t)$, $e_2(t)$, $e_3(t)$ and $e_4(t)$ asymptotically converge to zero as $t \to \infty$. $\diamondsuit$

It should be noted that since the errors $e_1(t)$, $e_2(t)$, $e_3(t)$ and $e_4(t)$ asymptotically converge to zero as $t \to \infty$, then we are guaranteed that $x_s(t)$, $y_s(t)$, $z_s(t)$, $w_s(t)$ asymptotically converge to $x_m(t)$, $y_m(t)$, $z_m(t)$, $w_m(t)$ respectively as $t \to \infty$. Therefore, it can be concluded that the states of the master and the states of the slave hyperchaotic L$\ddot{u}$ systems are synchronized.

Simulation Results

The performance of the system is studied through simulations. The master system given in (2) and the slave system given in (3) with the feedback linearization controller (5) are simulated using the Matlab software. The parameters of the Lü systems are taken such that $a = 36$, $b = 3$, $c = 20$ and $r = 1$. The parameters of the controller are such that $\gamma_1 = 1$ and $\gamma_2 = 1$. The initial conditions are taken to be $x_m(0) = -2$, $x_s(0) = 1$, $y_m(0) = 4$, $y_s(0) = -1$, $z_m(0) = 3$, $z_s(0) = 1$, $w_m(0) = 2$ and $w_s(0) = 1$. In addition, for the first five seconds of the simulations, the two L$\ddot{u}$ systems are simulated with $u_1(t) = u_2(t) = u_3(t) = 0$. Then for the next five seconds the control laws given by equations (5) are applied.

The simulation results are shown in Figure 2 -Figure 5. Figure 2 depicts $x_m(t)$ and $x_s(t)$ versus time; Figure 3 shows $y_m(t)$ and $y_s(t)$ versus time. Figure 4 shows $z_m(t)$ and $z_s(t)$ versus time and Figure 5 shows $w_m(t)$ and $w_s(t)$ versus time. These figures clearly indicate that the states of the master and the states of the slave systems are synchronized in less than 3 seconds. Therefore, the simulation results confirm that the feedback linearization control laws given by Theorem 1 are able to synchronize the master and slave hyperchaotic Lü systems starting from different initial conditions.

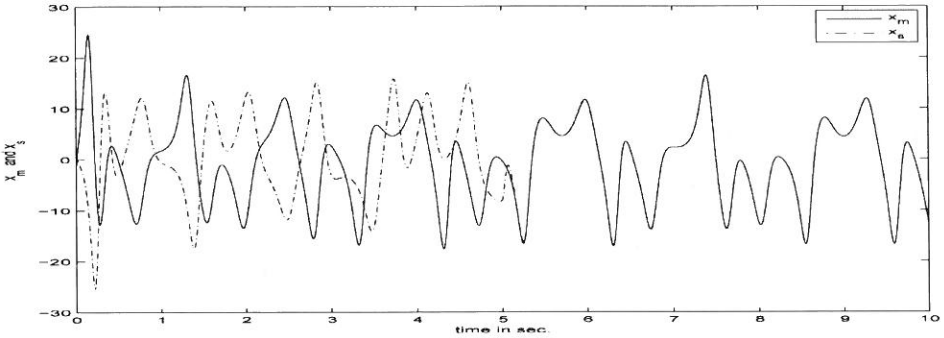

Fig. 2. The plots of x_m and x_s versus time using the Feedback Linearization controller (m = 3)

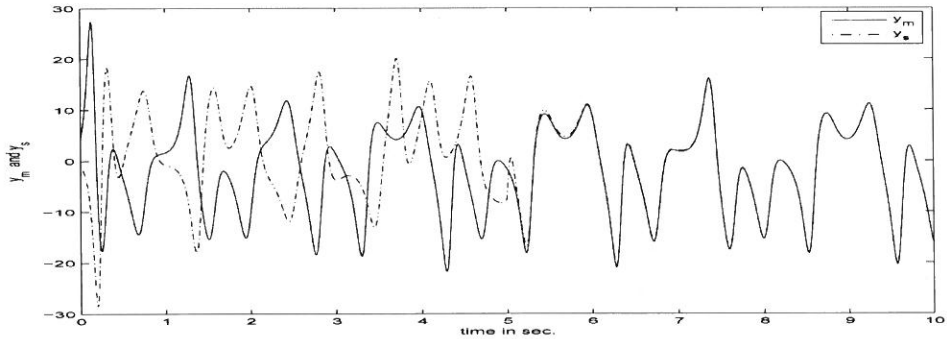

Fig.3. The plots of y_m and y_s versus time using the Feedback Linearization controller (m = 3)

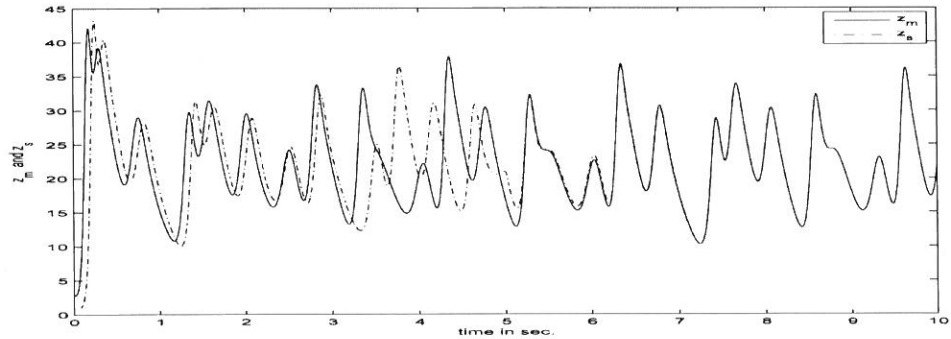

Fig. 4. The plots of z_m and z_s versus time using the Feedback Linearization controller (m = 3)

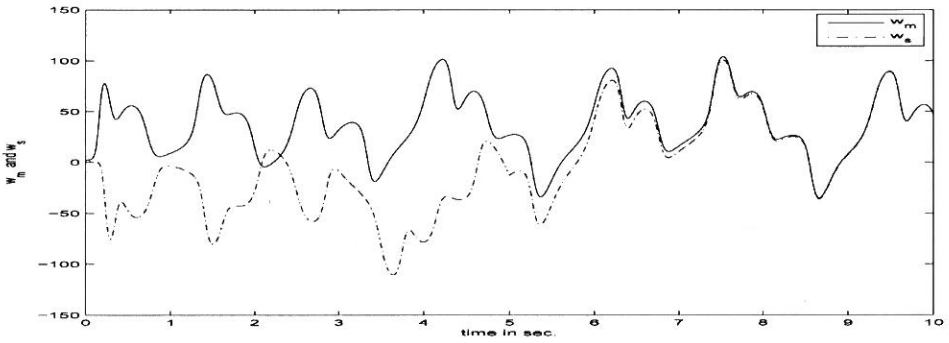

Fig. 5. The plots of w_m and w_s versus time using the Feedback Linearization controller (m = 3)

A SLIDING MODE CONTROLLER WHEN THE SLAVE SYSTEM HAS 3 INPUTS

Because of their robustness features, sliding mode controllers have been widely used to control different types of systems. In this section, we propose to use a sliding mode controller to synchronize two hyperchaotic Lü systems when the slave system has three inputs.

Design of the the Sliding Mode Controller

The first step in designing a sliding mode controller is to choose the sliding surfaces. Since the slave system has three inputs, we need to choose three sliding surfaces.

Let K_1, K_2, K_3, Γ_1, Γ_2 and Γ_3 be positive scalars. The sliding surfaces S_1, S_2 and S_3 are chosen such that:

$$\begin{aligned} S_1 &= e_2(t) \\ S_2 &= e_4(t) \\ S_3 &= e_3(t) \end{aligned} \tag{8}$$

Also, we define the *sign* function such that:

$$sgn(S) = \begin{cases} 1 & if\ S > 0 \\ 0 & if\ S = 0 \\ -1 & if\ S < 0 \end{cases}$$

Theorem 2: The sliding mode control laws:

$$\begin{aligned} u_1(t) &= x_s(t)e_3(t) + z_m(t)e_1(t) - ce_2(t) - K_1S_1 - \Gamma_1 sgn(S_1) \\ u_2(t) &= -x_s(t)e_3(t) - z_m(t)e_1(t) - re_4(t) - K_2S_2 - \Gamma_2 sgn(S_2) \\ u_3(t) &= -x_s(t)e_2(t) - y_m(t)e_1(t) + be_3(t) - K_3S_3 - \Gamma_3 sgn(S_3) \end{aligned} \tag{9}$$

when applied to the error system (4) guarantee the convergence of the errors $e_i(t)$ $(i = 1, ..., 4)$ to zero as t tends to infinity.

Proof:

Taking the time derivatives of S_1, S_2 and S_3 in (8) and using the dynamic model of the errors in (4) and the control laws given by (9), we obtain:

$$\begin{aligned} \dot{S}_1 &= -x_s(t)e_3(t) - z_m(t)e_1(t) + ce_2(t) + u_1(t) \\ &= -K_1S_1 - \Gamma_1 sgn(S_1) \end{aligned} \tag{10}$$

$$\begin{aligned} \dot{S}_2 &= x_s(t)e_3(t) + z_m(t)e_1(t) + re_4(t) + u_2(t) \\ &= -K_2S_2 - \Gamma_2 sgn(S_2) \end{aligned} \tag{11}$$

$$\begin{aligned} \dot{S}_3 &= x_s(t)e_2(t) + y_m(t)e_1(t) - be_3(t) + u_3(t) \\ &= -K_3S_3 - \Gamma_3 sgn(S_3) \end{aligned} \tag{12}$$

From (10)-(12), we conclude that $\dot{S}_i = -K_iS_i - \Gamma_i sgn(S_i)$ for $i = 1, 2, 3$. It can be easily checked that the equations given by (10)-(12) guarantee that $S_i\dot{S}_i < 0$ for $i = 1, 2, 3$. Therefore, the trajectories associated with these discontinuous dynamics exhibit a finite time reachability to zero from any given initial conditions provided that the gains K_1, K_2, K_3, Γ_1, Γ_2 and Γ_3 are chosen to be sufficiently large, strictly positive scalars.

Since S_1, S_2 and S_3 are driven to zero in finite time, then the errors $e_2(t)$, $e_3(t)$ and $e_4(t)$ are driven to zero in finite time. Moreover, since $e_2(t)$ and $e_4(t)$ are driven to zero in finite time, then after such a finite time, the first ode equation of the slave system (4) is such $\dot{e}_1(t) = -ae_1(t)$. Thus, $e_1(t)$ asymptotically converges to zero as $t \to \infty$ since a is a positive scalar. Therefore, the errors $e_1(t)$, $e_2(t)$, $e_3(t)$ and $e_4(t)$ converge to zero as $t \to \infty$. $\diamondsuit$

It should be noted that since the errors converge to zero as $t \to \infty$, then we are guaranteed that $x_s(t)$, $y_s(t)$, $z_s(t)$, $w_s(t)$ converge to $x_m(t)$, $y_m(t)$, $z_m(t)$, $w_m(t)$ respectively as $t \to \infty$. Hence, the states of the master and the states of the slave hyperchaotic Lü systems are synchronized.

Remark:

It is well known that sliding mode controllers suffer from the problem of undesired chattering. This problem can be greatly reduced by replacing the sign function with a saturation function such that:

$$Sat(S) = \begin{cases} 1 & if\ S > B_L \\ \dfrac{S}{B_L} & if\ |S| \leq B_L \\ -1 & if\ S < -B_L \end{cases}$$

where B_L is the thickness of the boundary layer.

Simulation Results

The master system given by (2) and the slave system given by (3) with the sliding mode controller given by (9) are simulated using the Matlab software. The parameters of the Lü systems as well as the initial conditions are the same as the ones given in the previous section. The parameters of the controller are taken to be $K_1 = K_2 = K_3 = 1$, $\Gamma_1 = 10$, $\Gamma_2 = 20$ and $\Gamma_3 = 10$. Also, for the first five seconds of the simulations, the two hyperchaotic Lü systems are simulated with $u_1(t) = u_2(t) = u_3(t) = 0$. Then for the next five seconds the control law in (9) is applied.

The simulation results are given in Figure 6 -Figure 9. Figure 6 depicts $x_m(t)$ and $x_s(t)$ versus time; Figure 7 shows $y_m(t)$ and $y_s(t)$ versus time. Figure 8 shows $z_m(t)$ and $z_s(t)$ versus time and Figure 9 shows $w_m(t)$ and $w_s(t)$ versus time. These figures clearly indicate that the states of the master and the states of the slave hyperchaotic Lü systems are synchronized in in less than 2 seconds. Therefore, the simulation results confirm that the sliding mode controller given by Theorem 2 is able to synchronize two hyperchaotic Lü systems starting from different initial conditions.

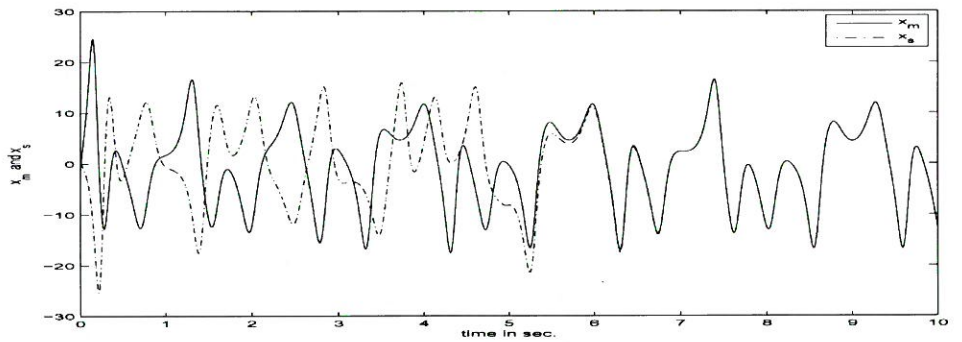

Fig. 6. The plots of x_m and x_s versus time using the Sliding Mode controller (m = 3)

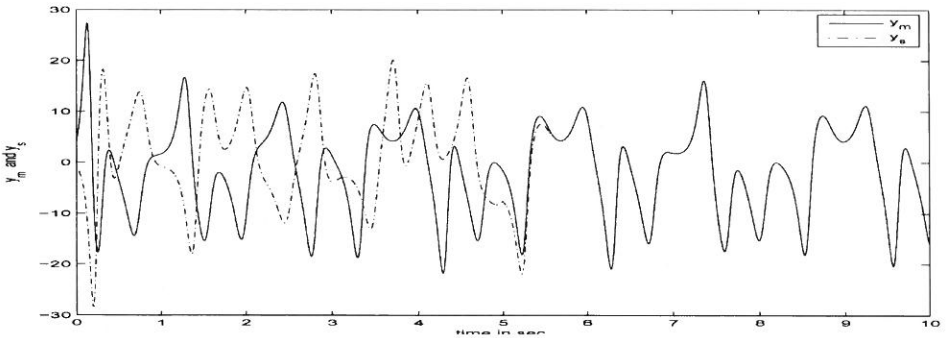

Fig. 7. The plots of y_m and y_s versus time using the Sliding Mode controller (m = 3)

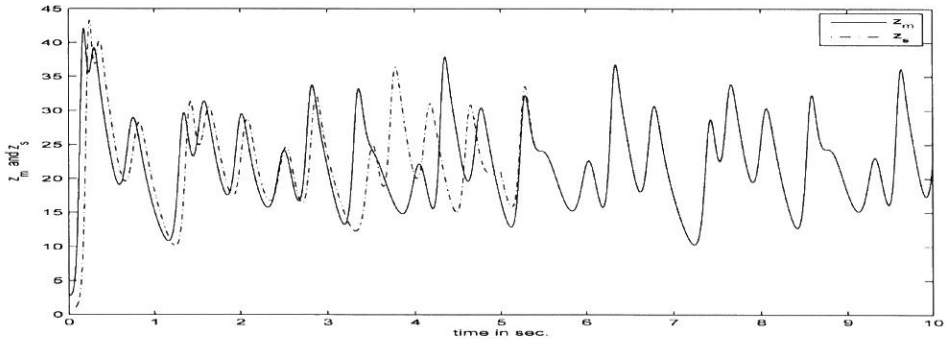

Fig. 8. The plots of z_m and z_s versus time using the Sliding Mode controller (m = 3)

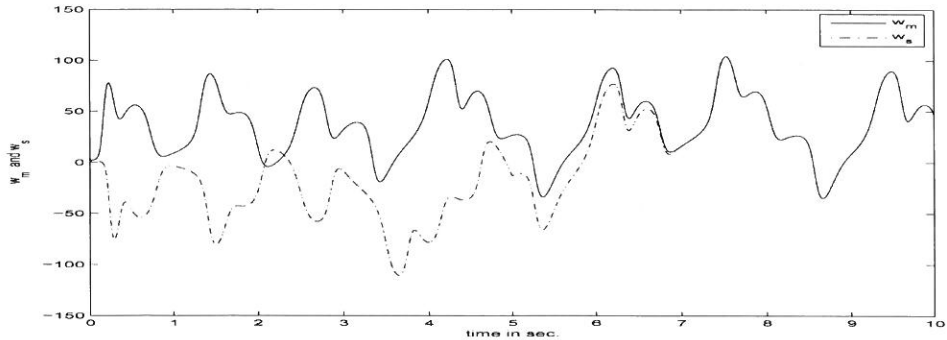

Fig. 9. The plots of w_m and w_s versus time using the Sliding Mode controller (m = 3)

A FEEDBACK LINEARIZATION CONTROLLER WHEN THE SLAVE SYSTEM HAS 2 INPUTS

It is assumed in the previous two sections that the slave Lü system has three inputs. From an implementation point view, it is desired to minimize the number of inputs. Therefore, we will assume in this section and in the next section that the slave system has two control inputs only (i.e. we will assume that $u_3 = 0$ in system (3)). Therefore, the dynamic model of the errors between the master and slave systems can be written as follows:

$$\begin{cases} \dot{e}_1(t) = a(e_2(t) - e_1(t)) + e_4(t) \\ \dot{e}_2(t) = -x_s(t)e_3(t) - z_m(t)e_1(t) + ce_2(t) + u_1(t) \\ \dot{e}_3(t) = x_s(t)e_2(t) + y_m(t)e_1(t) - be_3(t) \\ \dot{e}_4(t) = x_s(t)e_3(t) + z_m(t)e_1(t) + re_4(t) + u_2(t) \end{cases} \tag{13}$$

To facilitate the design of the control laws, we will define the following state transformation:

$$\begin{cases} \xi_1(t) = e_1(t) \\ \xi_2(t) = -ae_1(t) + ae_2(t) + e_4(t) \\ \xi_3(t) = e_3(t) \\ \xi_4(t) = x_s(t)e_2(t) + y_m(t)e_1(t) - be_3(t) \end{cases} \tag{14}$$

We will let the vector $\xi(t)$ be such that $\xi(t) = [\xi_1(t) \;\; \xi_2(t) \;\; \xi_3(t) \;\; \xi_4(t)]^T$.

Notice that if $x_s(t) \neq 0$, then the above transformation in invertible such that:

$$\begin{cases} e_1(t) = \xi_1(t) \\ e_2(t) = \dfrac{1}{x_s(t)}(\xi_4(t) - y_m(t)\xi_1(t) + b\xi_3(t)) \\ e_3(t) = \xi_3(t) \\ e_4(t) = \xi_2(t) + a\xi_1(t) - \dfrac{a}{x_s(t)}(\xi_4(t) - y_m(t)\xi_1(t) + b\xi_3(t)) \end{cases} \tag{15}$$

Using the transformation given in (14), the error dynamics between the master and slave systems in (13) can be written in the new coordinates as follows:

$$\begin{cases} \dot{\xi}_1(t) = \xi_2(t) \\ \dot{\xi}_2(t) = f_1 + v_1(t) \\ \dot{\xi}_3(t) = \xi_4(t) \\ \dot{\xi}_4(t) = f_2 + v_2(t) \end{cases} \tag{16}$$

where,

$$v_1(t) = au_1(t) + u_2(t) \tag{17}$$

$$v_2(t) = x_s(t)u_1(t) \tag{18}$$

and,

$$\begin{aligned} f_1 \;=\; & a(-x_s(t)e_3(t) - z_m(t)e_1(t) + ce_2(t)) - a(ae_2(t) - ae_1(t) + e_4(t)) + x_s(t)e_3(t) \\ & + z_m(t)e_1(t) + re_4(t) \end{aligned} \tag{19}$$

$$\begin{aligned} f_2 \;=\; & (ay_s(t) - ax_s(t) + w_s(t))e_2(t) + (-x_s(t)e_3(t) - z_m(t)e_1(t) + ce_2(t))x_s(t) \\ & + (-x_m(t)z_m(t) + cy_m(t))e_1(t) + (ae_2(t) - ae_1(t) + e_4(t))y_m(t) \\ & - b(x_s(t)e_2(t) + y_m(t)e_1(t) - be_3(t)) \end{aligned} \tag{20}$$

Design of the the Controller

Let $\bar{\alpha}_1$, $\bar{\alpha}_2$, $\bar{\alpha}_3$, $\bar{\alpha}_4$, $\bar{\gamma}_1$ and $\bar{\gamma}_2$ be positive scalars. Also, let ϵ be a small positive scalar.

Theorem 3: The feedback linearization control laws:

$$u_1(t) = \begin{cases} -\dfrac{1}{x_s(t)}(f_2 + \bar{\alpha}_3 e_3(t) + \bar{\alpha}_4(x_s(t)e_2(t) + y_m(t)e_1(t) - be_3(t))) & \text{if } |x_s(t)| > \epsilon \\ x_s(t)e_3(t) + z_m(t)e_1(t) - (c + \bar{\gamma}_1)e_2(t) & \text{if } |x_s(t)| \le \epsilon \end{cases} \tag{21}$$

$$u_2(t) = \begin{cases} -(f_1 + \bar{\alpha}_1 e_1(t) + \bar{\alpha}_2(-ae_1(t) + ae_2(t) + e_4(t))) \\ \quad + \dfrac{a}{x_s(t)}(f_2 + \bar{\alpha}_3 e_3(t) + \bar{\alpha}_4(x_s(t)e_2(t) + y_m(t)e_1(t) - be_3(t))) & \text{if } |x_s(t)| > \epsilon \\ -x_s(t)e_3(t) - z_m(t)e_1(t) - (r + \bar{\gamma}_2)e_4(t) & \text{if } |x_s(t)| \le \epsilon \end{cases} \tag{22}$$

when applied to the error system in (13) guarantee the asymptotic convergence of the errors $e_i(t)$ $(i = 1, ..., 4)$ to zero as t tends to infinity.

Proof:

Since the control laws in (21)-(22) are defined for $|x_s(t)| \leq \epsilon$ differently from the case when $|x_s(t)| > \epsilon$, the proof is divided into two cases.

Case 1: $|x_s(t)| > \epsilon$

The closed loop system when the feedback linearization controller (21)-(22) is applied to the error system given by equation (16) is such:

$$\dot{\xi}(t) = A_c\xi(t) \tag{23}$$

where,

$$A_c = \begin{bmatrix} 0 & 1 & 0 & 0 \\ -\bar{\alpha}_1 & -\bar{\alpha}_2 & 0 & 0 \\ 0 & 0 & 0 & 1 \\ 0 & 0 & -\bar{\alpha}_3 & -\bar{\alpha}_4 \end{bmatrix}.$$

The solution of the equation given in (23) is $\xi(t) = exp(A_c t)\xi(0)$ for $t \geq 0$. It can be easily checked that the matrix A_c is a stable matrix as $\bar{\alpha}_1$, $\bar{\alpha}_2$, $\bar{\alpha}_3$, $\bar{\alpha}_4$ are positive scalars. Hence, $\xi(t)$ asymptotically converges to zero as $t \to \infty$.

Because the transformation (14) is invertible when $x_s(t) \neq 0$, and since $\xi(t)$ asymptotically converges to zero as $t \to \infty$, then the errors $e_1(t)$, $e_2(t)$, $e_3(t)$, $e_4(t)$ will also asymptotically converge to zero as $t \to \infty$.

Case 2: $|x_s(t)| \leq \epsilon$

In this case, the application of the controller in (21) to the second ode of the error system given in (13) leads to the first order ode $\dot{e}_2 = -\bar{\gamma}_1 e_2(t)$; the solution of this ode is $e_2(t) = exp(-\bar{\gamma}_1 t)e_2(0)$. Since the scalar $\bar{\gamma}_1$ is greater than 0, then the asymptotic convergence of $e_2(t)$ to zero as $t \to \infty$ is guaranteed. Also, the application of the controller in (22) to the fourth ode of the error system given in (13) leads to the first order ode $\dot{e}_4 = -\bar{\gamma}_2 e_4(t)$; the solution of this ode is $e_4(t) = exp(-\bar{\gamma}_2 t)e_4(0)$. Again, since the scalar $\bar{\gamma}_2$ is greater than 0, then the asymptotic convergence of $e_4(t)$ to zero as $t \to \infty$ is guaranteed. Moreover, since $e_2(t)$ and $e_4(t)$ asymptotically converge to zero, then the first ode of the error system given in (13) leads to the asymptotic convergence of $e_1(t)$ to zero as $t \to \infty$ as a is a positive scalar. Finally, since $e_1(t)$ and $e_2(t)$ asymptotically converge to zero and because $x_s(t)$ and $y_m(t)$ are bounded, then the third ode of the error system given in (13) leads to the asymptotic convergence of $e_3(t)$ to zero as $t \to \infty$ as b is a positive scalar.

Therefore, it can be concluded that for all values of $x_s(t)$, the errors asymptotically converge to zero as $t \to \infty$. $\diamondsuit$

Hence, it can be concluded that the states of the master and the slave hyperchaotic Lü systems are synchronized.

Simulation Results

The master system given in (2) and the slave system given in (3) with $u_3 = 0$ and using the feedback linearization controller (21)-(22) are simulated using the Matlab software. The parameters of the hyperchaotic Lü systems as well as the initial conditions are the same as the ones given above. The parameters of the controller are chosen such that $\bar{\alpha}_1 = 110$, $\bar{\alpha}_2 = 21$, $\bar{\alpha}_3 = 110$, $\bar{\alpha}_4 = 21$, $\bar{\gamma}_1 = 5$ and $\bar{\gamma}_2 = 5$.

The simulation results are presented in Figure 10 - Figure 13. Figure 10 depicts $x_m(t)$ and $x_s(t)$ versus time; Figure 11 shows $y_m(t)$ and $y_s(t)$ versus time. Figure 12 depicts $z_m(t)$ and $z_s(t)$ versus time and Figure 13 shows $w_m(t)$ and $w_s(t)$ versus time. These figures clearly indicate that the errors asymptotically converge to zero as $t \to \infty$. Therefore, the simulation results confirm that the feedback linearization control laws given by Theorem 3 are able to synchronize the two hyperchaotic Lü systems starting from different initial conditions.

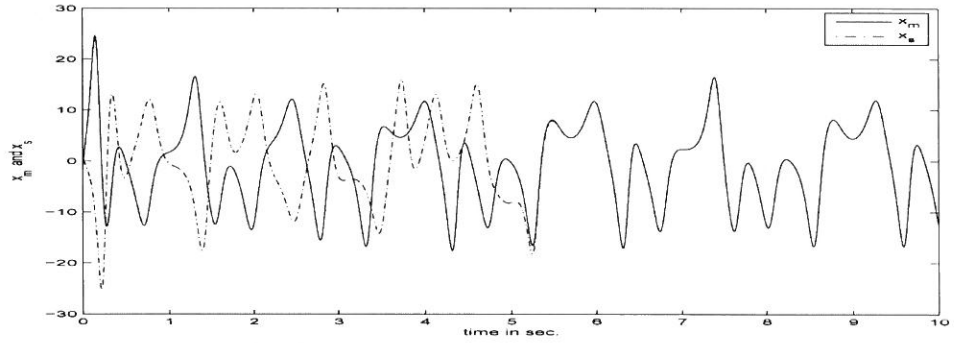

Fig. 10. The plots of x_m and x_s versus time using the Feedback Linearization controller (m = 2)

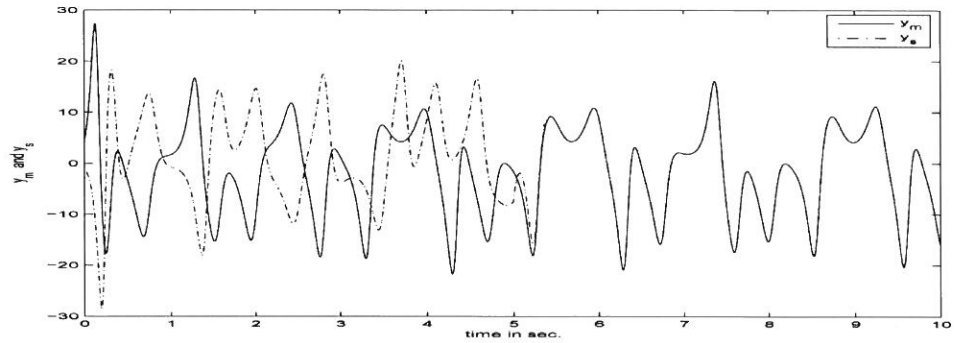

Fig. 11. The plots of y_m and y_s versus time using the Feedback Linearization controller (m = 2)

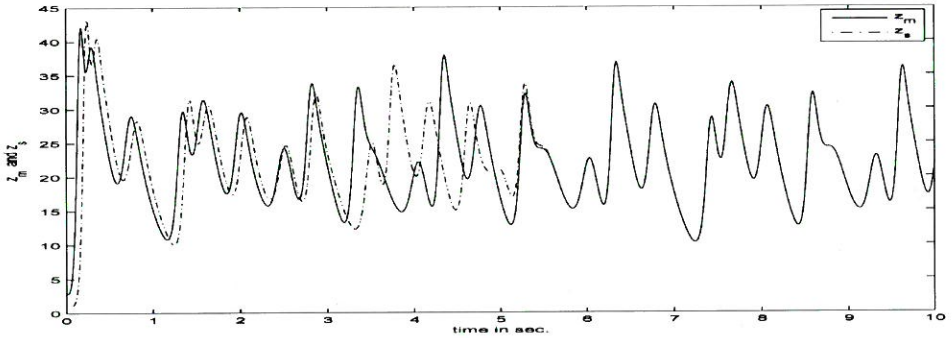

Fig. 12. The plots of z_m and z_s versus time using the Feedback Linearization controller (m = 2)

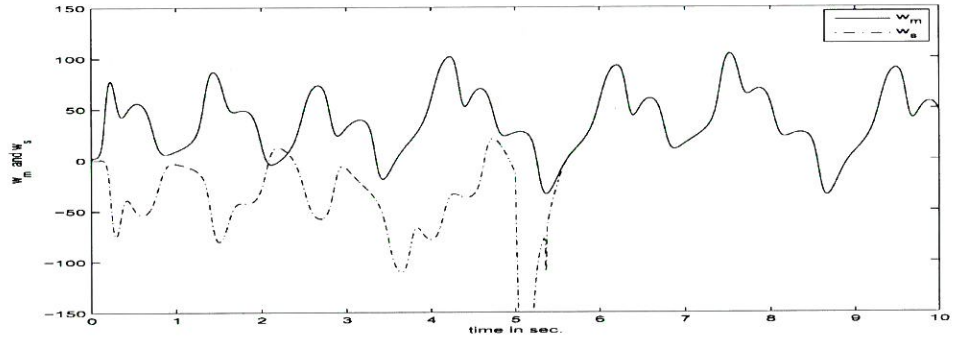

Fig. 13. The plots of w_m and w_s versus time using the Feedback Linearization controller (m = 2)

A SLIDING MODE CONTROLLER WHEN THE SLAVE SYSTEM HAS 2 INPUTS

Design of the the Sliding Mode Controller

Let $\bar{\beta}_1$, $\bar{\beta}_2$, $\bar{K}_1$, $\bar{K}_2$, $\bar{K}_3$, $\bar{K}_4$, $\bar{\Gamma}_1$, $\bar{\Gamma}_2$, $\bar{\Gamma}_3$ and $\bar{\Gamma}_4$ be positive scalars. Also, let ϵ be a small positive scalar.

Define the sliding surfaces σ_1 and σ_2 such that,

$$\sigma_1 = \xi_2(t) + \bar{\beta}_1 \xi_1(t) \tag{24}$$

$$\sigma_2 = \xi_4(t) + \bar{\beta}_2 \xi_3(t) \tag{25}$$

where $\xi_i(t)$ (i = 1,...,4) are given by equations (14).

Theorem 4: The sliding mode control laws:

$$u_1(t) = \begin{cases} -\dfrac{1}{x_s(t)}\left(f_2 + \bar{\beta}_2\xi_4 + \bar{K}_2\sigma_2 + \bar{\Gamma}_2 sgn(\sigma_2)\right) & if\ |x_s(t)| > \epsilon \\ x_s(t)e_3(t) + z_m(t)e_1(t) - ce_2(t) - \bar{K}_3e_2(t) - \bar{\Gamma}_3 sgn(e_2(t)) & if\ |x_s(t)| \leq \epsilon \end{cases} \tag{26}$$

$$u_2(t) = \begin{cases} -f_1 - \bar{\beta}_1\xi_2 - \bar{K}_1\sigma_1 - \bar{\Gamma}_1 sgn(\sigma_1) + ax_s(t)\left(f_2 + \bar{\beta}_2\xi_4 + \bar{K}_2\sigma_2 + \bar{\Gamma}_2 sgn(\sigma_2)\right) & if\ |x_s(t)| > \epsilon \\ -x_s(t)e_3(t) - z_m(t)e_1(t) - re_4(t) - \bar{K}_4e_4(t) - \bar{\Gamma}_4 sgn(e_4(t)) & if\ |x_s(t)| \leq \epsilon \end{cases} \tag{27}$$

with,

$$\xi_2(t) = -ae_1(t) + ae_2(t) + e_4(t) \tag{28}$$

$$\xi_4(t) = x_s(t)e_2(t) + y_m(t)e_1(t) - be_3(t) \tag{29}$$

when applied to the error system system (13) guarantee the convergence of the errors $e_i(t)$ $(i = 1, ..., 4)$ to zero as t tends to infinity.

Proof:

Since the control laws in (26)-(29) are defined for $|x_s(t)| > \epsilon$ differently from the case when $|x_s(t)| \leq \epsilon$, the proof is divided into two cases.

Case 1: $|x_s(t)| > \epsilon$

Taking the time derivative of σ_1 and σ_2 and using the error dynamics (16) and the control laws given by (26)-(29), we obtain:

$$\begin{aligned} \dot{\sigma}_1 &= \bar{\beta}_1\dot{\xi}_1(t) + \dot{\xi}_2(t) \\ &= \bar{\beta}_1\xi_2(t) + f_1 + au_1(t) + u_2(t) \\ &= \bar{\beta}_1\xi_2(t) + f_1 - \frac{a}{x_s(t)}\left(f_2 + \bar{\beta}_2\xi_4(t) + \bar{K}_2\sigma_2 + \bar{\Gamma}_2 sgn(\sigma_2)\right) \\ &\quad -f_1 - \bar{\beta}_1\xi_2(t) - \bar{K}_1\sigma_1 - \bar{\Gamma}_1 sgn(\sigma_1) + \frac{a}{x_s(t)}\left(f_2 + \bar{\beta}_2\xi_4(t) + \bar{K}_2\sigma_2 + \bar{\Gamma}_2 sgn(\sigma_2)\right) \\ &= -\bar{K}_1\sigma_1 - \bar{\Gamma}_1 sgn(\sigma_1) \end{aligned} \tag{30}$$

Also,

$$\begin{aligned}\dot{\sigma}_2 &= \bar{\beta}_2\dot{\xi}_3(t) + \dot{\xi}_4(t) \\ &= f_2 + \bar{\beta}_2\xi_4(t) + x_s(t)u_1(t) \\ &= f_2 + \bar{\beta}_2\xi_4(t) - (f_2 + \bar{\beta}_2\xi_4(t) + \bar{K}_2\sigma_2 + \bar{\Gamma}_2 sgn(\sigma_2)) \\ &= -\bar{K}_2\sigma_2 - \bar{\Gamma}_2 sgn(\sigma_2)\end{aligned} \tag{31}$$

We can conclude from (30)-(31) that $\dot{\sigma}_i = -\bar{K}_i\sigma_i - \bar{\Gamma}_i sgn(\sigma_i)$ for $i = 1, 2$. It can be easily checked that the conditions given by (30)-(31) guarantee that $\sigma_i\dot{\sigma}_i < 0$ for $i = 1, 2$. Therefore, the trajectories associated with these discontinuous dynamics exhibit a finite time reachability to zero from any given initial conditions provided that the gains $\bar{K}_1$, $\bar{K}_2$, $\bar{\Gamma}_1$ and $\bar{\Gamma}_2$ are chosen to be sufficiently large, strictly positive scalars.

Since σ_1 is driven to zero in finite time, then after such a finite time we have $\sigma_1 = 0$, or

$$\xi_2 = -\bar{\beta}_1\xi_1 \tag{32}$$

After such a finite time, the first ode equation of the error dynamics (16) is such that $\dot{\xi}_1(t) = -\bar{\beta}_1\xi_1(t)$; the solution of this ode is $\xi_1(t) = exp(-\bar{\beta}_1 t)\xi_1(0)$. Thus, $\xi_1(t)$ asymptotically converges to zero as $t \to \infty$ since $\bar{\beta}_1$ is a positive scalar. Moreover, Since σ_1 is driven to zero in finite time and since $\xi_1(t)$ asymptotically converges to zero, then it can be concluded that $\xi_2(t)$ asymptotically converges to zero as $t \to \infty$.

Also, since σ_2 is driven to zero in finite time, then after such a finite time we have $\sigma_2 = 0$, or

$$\xi_4(t) = -\bar{\beta}_2\xi_3(t) \tag{33}$$

After such a finite time, the third ode equation of the error dynamics (16) is such that $\dot{\xi}_3(t) = -\bar{\beta}_2\xi_3(t)$; the solution of this ode is $\xi_3(t) = exp(-\bar{\beta}_2 t)\xi_3(0)$. Thus, $\xi_3(t)$ asymptotically converges to zero as $t \to \infty$ since $\bar{\beta}_2$ is a positive scalar. Moreover, Since σ_2 is driven to zero in finite time and since $\xi_3(t)$ asymptotically converges to zero, then it can be concluded that $\xi_4(t)$ asymptotically converges to zero as $t \to \infty$.

Thus, it can be concluded that the sliding mode controller (26)-(29) when applied to the hyperchaotic Lü system guarantees the asymptotic convergence of $\xi_1(t)$, $\xi_2(t)$, $\xi_3(t)$ and $\xi_4(t)$ to zero as $t \to \infty$. Furthermore, because the transformation (14) is invertible when $x_s(t) \neq 0$, and since $\xi(t)$ converges to zero

as $t \to \infty$, then the errors $e_1(t)$, $e_2(t)$, $e_3(t)$, $e_4(t)$ will also asymptotically converge to zero as $t \to \infty$.

Case 2: $|x_s(t)| \leq \epsilon$

The application of the controller in (26) to the second ode of the error system given by (13) leads to:

$$\dot{e}_2(t) = -\bar{K}_3 e_2(t) - \bar{\Gamma}_3 sgn(e_2(t)) \tag{34}$$

Also, the application of the controller in (27) to the fourth ode of the error system given by (13) leads to:

$$\dot{e}_4(t) = -\bar{K}_4 e_4(t) - \bar{\Gamma}_4 sgn(e_4(t)) \tag{35}$$

It can be easily checked that the equations given by (34)-(35) guarantee that $e_2(t)\dot{e}_2(t) < 0$ and $e_4(t)\dot{e}_4(t) < 0$. The trajectories associated with these discontinuous dynamics (34)-(35) exhibit a finite time reachability to zero from any given initial conditions provided that the constant gains $\bar{K}_3$, $\bar{K}_4$, $\bar{\Gamma}_3$, $\bar{\Gamma}_4$ are chosen to be sufficiently large, strictly positive scalars. Therefore $e_2(t)$ and $e_4(t)$ are driven to zero in finite time. Moreover, since $e_2(t)$ and $e_4(t)$ converge to zero, then the first ode of the error system given in (13) leads to the asymptotic convergence of $e_1(t)$ to zero as $t \to \infty$ since the scalar a is greater than 0. Finally, since $e_1(t)$ and $e_2(t)$ converge to zero and because $x_s(t)$ and $y_m(t)$ are bounded, then the third ode of the error system given in (13) leads to the asymptotic convergence of $e_3(t)$ to zero as $t \to \infty$ since b is a positive scalar.

Hence for all values of $x_s(t)$, the errors $e_1(t)$, $e_2(t)$, $e_3(t)$, $e_4(t)$ converge to zero as $t \to \infty$. $\diamondsuit$

Therefore, we are guaranteed that the states of the master and the slave hyperchaotic Lü systems are synchronized.

Simulation Results

The master system given in (2) and the slave system given in (3) with $u_3 = 0$ and using the sliding mode controller (26)-(29) are simulated using the Matlab software. The parameters of the Lü systems as well as the initial conditions are the same as the ones given above. The parameters of the controller are chosen such that $\bar{K}_1 = \bar{K}_2 = \bar{K}_3 = \bar{K}_4 = 1$, $\bar{\beta}_1 = 5$, $\bar{\beta}_2 = 5$, $\bar{\Gamma}_1 = 100$, $\bar{\Gamma}_2 = 100$, $\bar{\Gamma}_3 = 10$ and $\bar{\Gamma}_4 = 10$.

The simulation results are given in Figure 14 - Figure 17. Figure 14 depicts $x_m(t)$ and $x_s(t)$ versus time; Figure 15 shows $y_m(t)$ and $y_s(t)$ versus time. Figure 16 depicts $z_m(t)$ and $z_s(t)$ versus time and Figure 17 shows $w_m(t)$ and $w_s(t)$

versus time. These figures clearly indicate that the errors asymptotically converge to zero as $t \to \infty$.

Therefore, the simulation results confirm that the sliding mode control law given by Theorem 4 is able to synchronize two hyperchaotic Lü systems starting from different initial conditions.

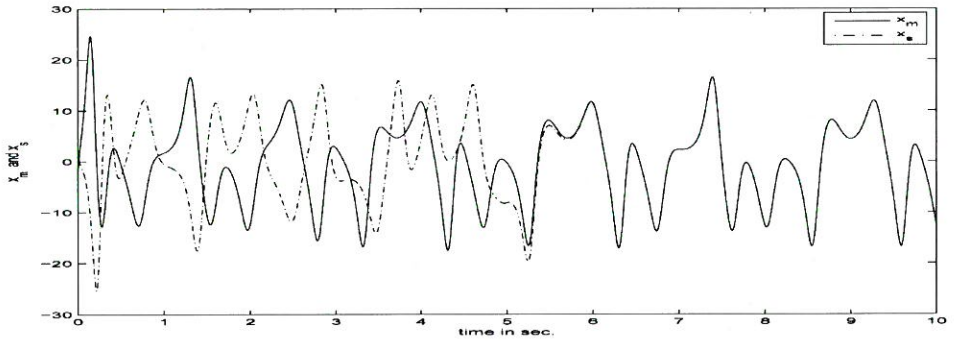

Fig. 14. The plots of x_m and x_s versus time using the Sliding Mode controller (m = 2)

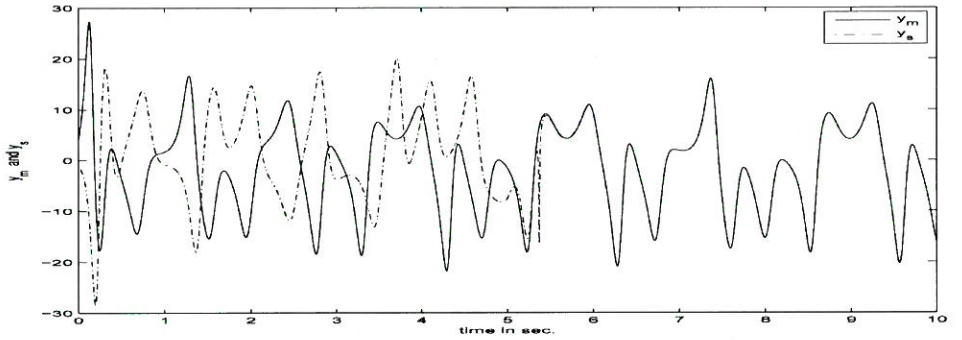

Fig. 15. The plots of y_m and y_s versus time using the Sliding Mode controller (m = 2)

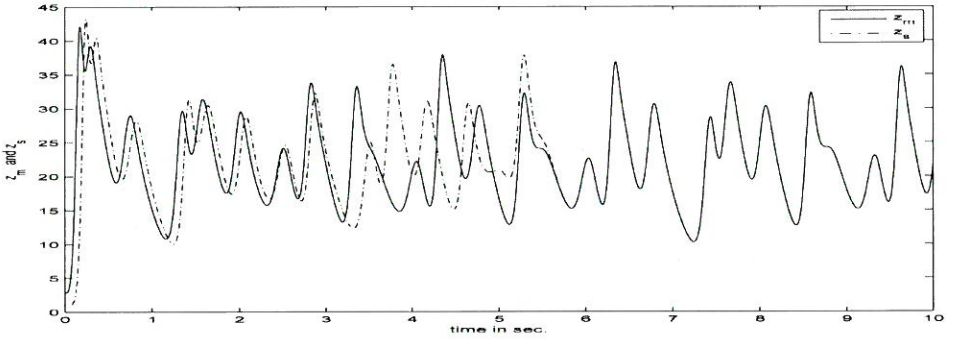

Fig. 16. The plots of z_m and z_s versus time using the Sliding Mode controller (m = 2)

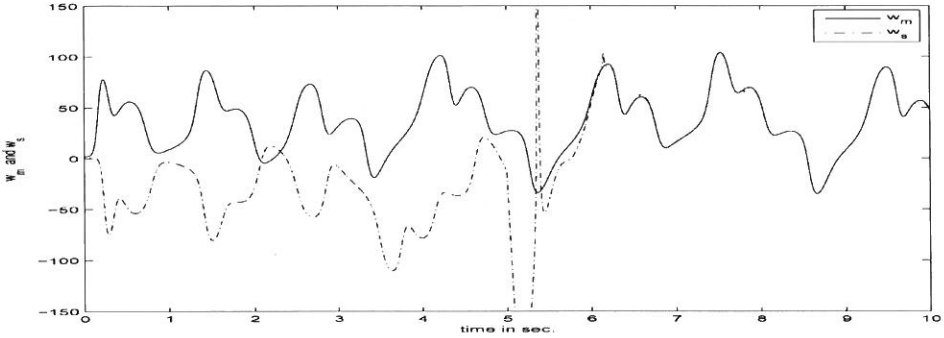

Fig. 17. The plots of w_m and w_s versus time using the Sliding Mode controller (m = 2)

APPLICATION OF THE PROPOSED CONTROL SCHEMES FOR SECURE COMMUNICATION

This section deals with the application of the proposed synchronization schemes for secure communications purposes. At first the secure communication procedure is described; then simulation results are presented when the four proposed control schemes are used.

Secure Communication Procedure

A secure communication procedure using the proposed control schemes is depicted in Figure 18.

The procedure is as follows:

1 - We have a hyperchaotic Lü system which is denoted as the master system at the transmitter side; this system is described using the the following differential equations:

$$\begin{cases} \dot{x}_m(t) = a(y_m(t) - x_m(t)) + w_m(t) \\ \dot{y}_m(t) = -x_m(t)z_m(t) + cy_m(t) \\ \dot{z}_m(t) = x_m(t)y_m(t) - bz_m(t) \\ \dot{w}_m(t) = x_m(t)z_m(t) + rw_m(t) \end{cases} \tag{36}$$

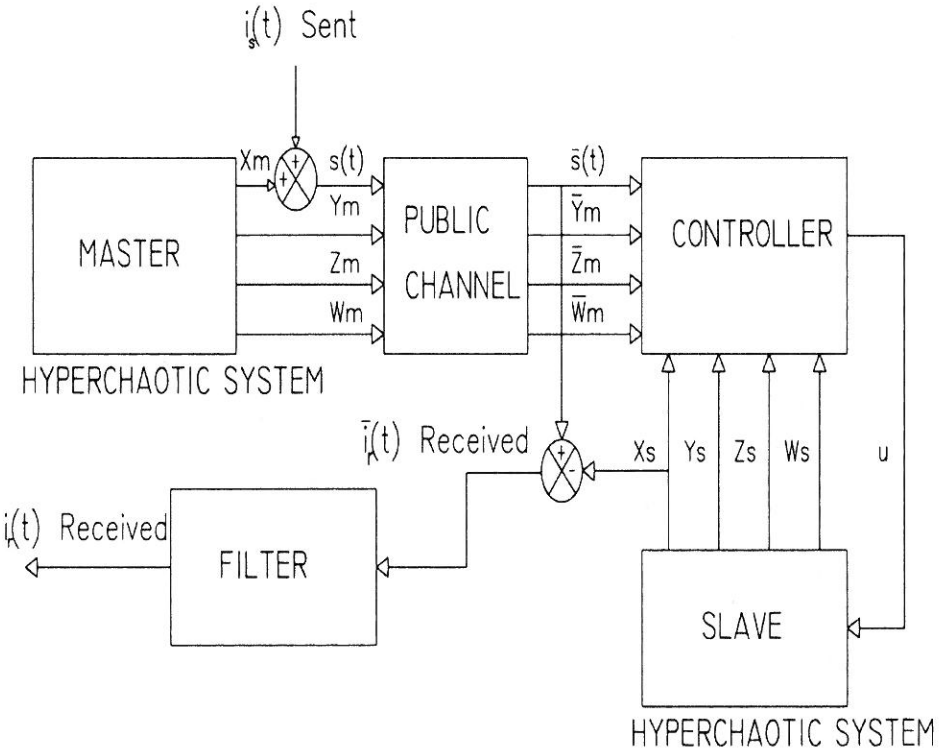

Fig. 18. Block diagram for the secure communication procedure

2 - We will assume that the message to be sent $i_s(t)$ is a binary signal which consists of a sequence of zeros and ones.

3 - We will add the information message $i_s(t)$ to the first state of the master system $x_m(t)$; the combined signal is denoted by $s(t)$.

4 - We will transmit the signals $s(t)$, $y_m(t)$, $z_m(t)$ and $w_m(t)$ using a public channel.

5 - Due to the presence of noise, the transmitted signals $s(t)$, $y_m(t)$ $z_m(t)$ and $w_m(t)$ will be corrupted with noise of the public channel. Therefore, the corrupted signals will be denoted by $\bar{s}(t)$, $\bar{y}_m(t)$, $\bar{z}_m(t)$ and $\bar{w}_m(t)$ respectively.

6 - We will use a hyperchaotic Lü system (the salve system) at the receiver side. The equations of this system are as follows:

$$\begin{cases} \dot{x}_s(t) = a(y_s(t) - x_s(t)) + w_s(t) \\ \dot{y}_s(t) = -x_s(t)z_s(t) + cy_s(t) + u_1(t) \\ \dot{z}_s(t) = x_s(t)y_s(t) - bz_s(t) + u_3(t) \\ \dot{w}_s(t) = x_s(t)z_s(t) + rw_s(t) + u_2(t) \end{cases} \tag{37}$$

7 - The developed control schemes will be used to synchronize the master and the slave systems. The errors between the states of the master and the slave systems are as follows: $\bar{e}_1(t) = x_s(t) - \bar{s}(t)$, $\bar{e}_2(t) = y_s(t) - \bar{y}_m(t)$, $\bar{e}_3(t) = z_s(t) - \bar{z}_m(t)$ and $\bar{e}_4(t) = w_s(t) - \bar{w}_m(t)$.

8 - To recover the transmitted message, we subtract the first state of the slave system $x_s(t)$ from the received signal $\bar{s}(t)$. The recovered signal is corrupted with some additive noise from the public channel.

9 - We can filter the recovered noisy signal to obtain exact transmitted information signal. We will use a filter's $F(.)$ such that:

$$i_r(t) = F(\bar{i}_r(t)) = F(\bar{s}(t) - x_s(t)) \tag{38}$$

where $i_s(t)$ is the sent information signal, $\bar{i}_r(t)$ is the received signal corrupted with noise. The signal $i_r(t)$ is the actual information signal after filtering.

It takes a small amount of time for the controller to synchronize the master and the slave systems when the sent signal has amplitude zero. Therefore, the filter is designed such that it will check the values of $\bar{s}(t) - x_s(t)$ every approximately 85% to 95% of each time period T in order to ensure that the synchronization is obtained whenever a signal $i_s(t)$ of amplitude zero is sent. Otherwise, the master and the slave systems are not synchronized and the output of the filter is a signal whose amplitude is one.

Secure Communications Using the Feedback Linearization Controller with m = 3

The feedback linearization controller (5) is used for secure communications. The performances of the controlled systems are simulated using the Matlab software. The initial conditions are the same as the ones given in section 3. The transmitted information $i_s(t)$ is a sequence of zeros and ones; note that the amplitude of the signal is scaled by a factor of 0.5.

Moreover, considering the fact that the information will be transmitted through a public channel, a Gaussian random signal is added to the transmitted signal. The added signal has a mean value of 0 and a variance of 0.01.

The simulation results are presented in Figures 19-20. Figure 19 depicts the plots of $x_m(t)$, $x_s(t)$ and $e(t)$ versus time using the feedback linearization controller when m = 3. Figure 20 shows the plots of $i_s(t)$ and $\bar{i}_s(t)$ versus time using the feedback linearization controller. Clearly, the simulation results indicate that the feedback linearization controller with m = 3 enables us to recover the sent message.

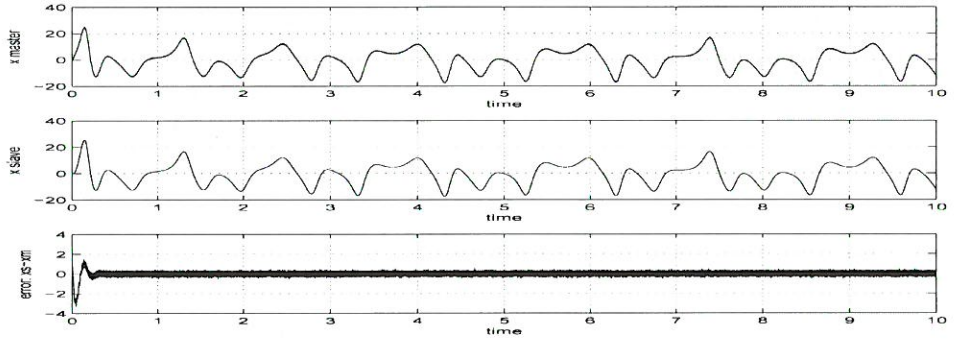

Fig. 19. The plots of x_m, x_s and e versus time using the Feedback Linearization controller (m = 3)

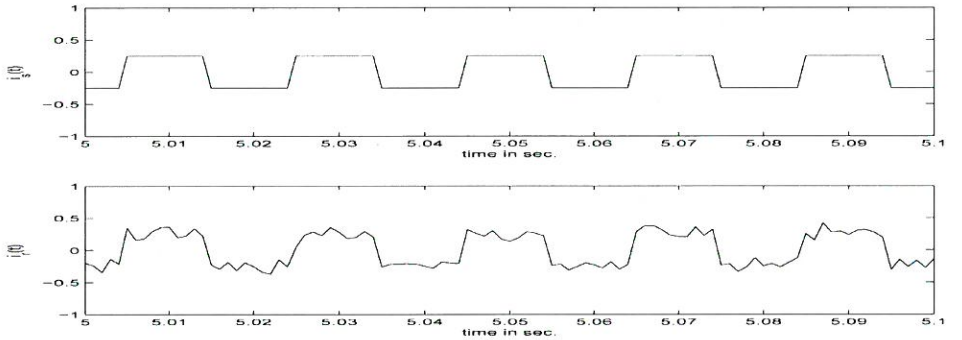

Fig. 20. The plots of $i_s(t)$ and $\bar{i}_s$ versus time using the Feedback Linearization controller (m = 3)

Secure Communications Using the Sliding Mode Controller with m = 3

The sliding mode controller (9) is used for secure communications. The simulation results are presented in Figures 21-22. Figure 21 depicts the plots of $x_m(t)$, $x_s(t)$ and $e(t)$ versus time using the sliding mode controller when m = 3. Figure 22 shows the plots of $i_s(t)$ and $\bar{i}_s(t)$ versus time using the sliding mode controller. Clearly, the simulation results indicate that the sliding mode controller with m = 3 enables us to recover the sent message.

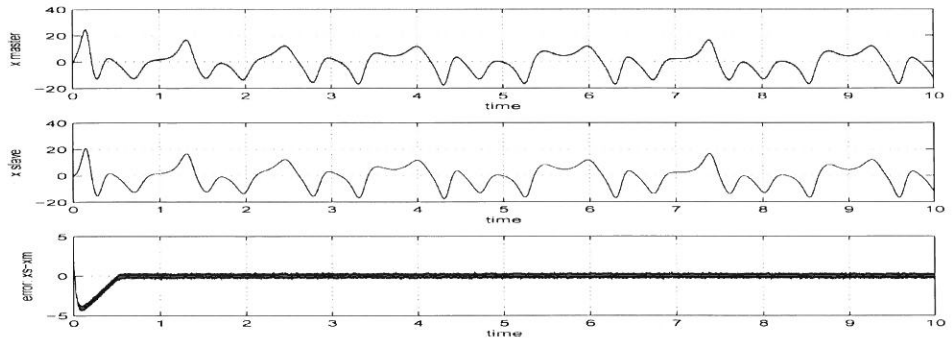

Fig. 21. The plots of x_m, x_s and e versus time using the Sliding Mode controller (m = 3)

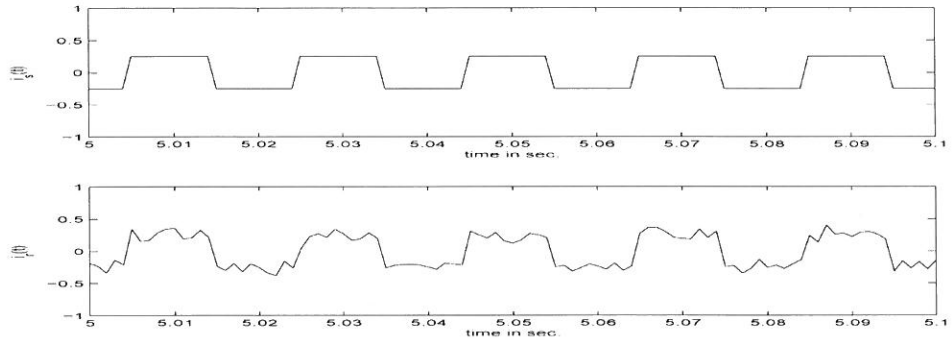

Fig. 22. The plots of $i_s(t)$ and $\bar{i}_s$ versus time using the Sliding Mode controller (m = 3)

Secure Communications Using the Feedback Linearization Controller with m = 2

The feedback linearization controller (21)-(22) is used for secure communications. The simulation results are presented in Figures 23-24. Figure 23 depicts the plots of $x_m(t)$, $x_s(t)$ and $e(t)$ versus time using the feedback linearization controller when m = 2. Figure 24 shows the plots of $i_s(t)$ and $\bar{i}_s(t)$ versus time using the feedback linearization controller. Clearly, the simulation results indicate that the FL controller with m = 2 enables us to recover the sent message.

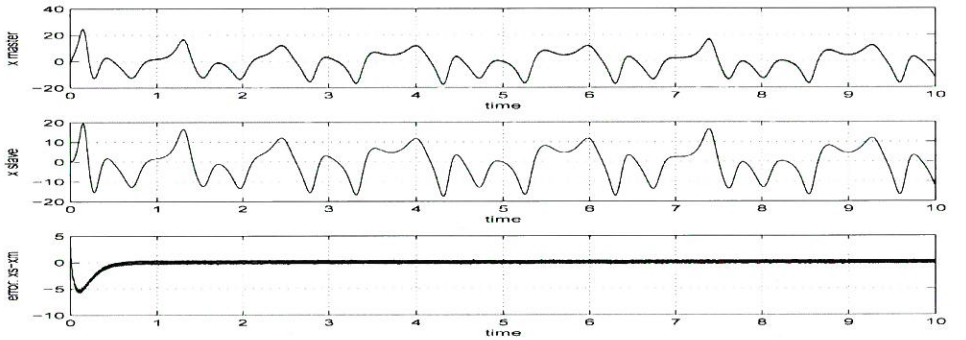

Fig. 23. The plots of x_m, x_s and e versus time using the Feedback Linearization controller (m = 2)

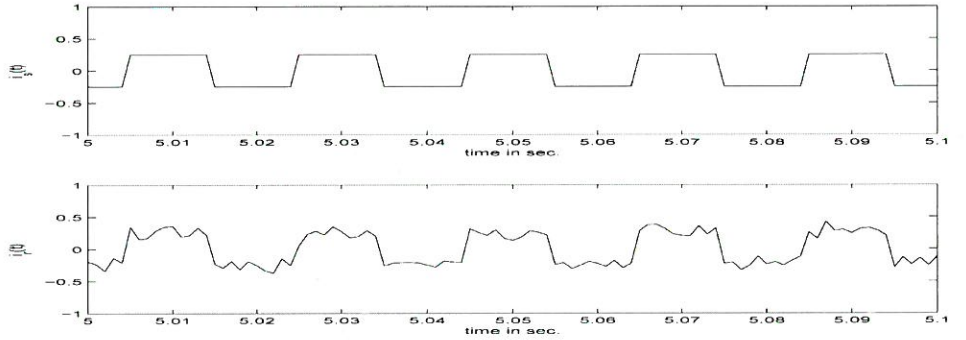

Fig. 24. The plots of $i_s(t)$ and $\bar{i}_s$ versus time using the Feedback Linearization controller (m = 2)

Secure Communications Using the Sliding Mode Controller with m = 2

The sliding mode controller (26)-(29) is used for secure communications. The simulation results are presented in Figures 25-26. Figure 25 depicts the plots of $x_m(t)$, $x_s(t)$ and $e(t)$ versus time using the sliding mode controller when m = 2. Figure 26 shows the plots of $i_s(t)$ and $\bar{i}_s(t)$ versus time using the sliding mode controller. Clearly, the simulation results indicate that the sliding mode controller with m = 2 enables us to recover the sent message.

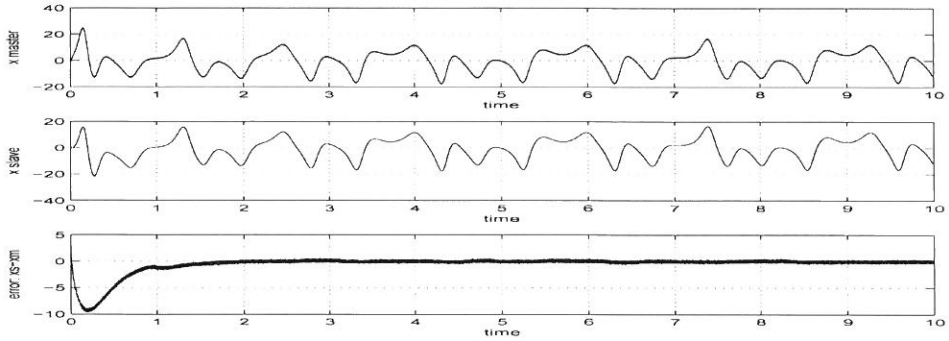

Fig. 25. The plots of x_m, x_s and e versus time using the Sliding Mode controller (m = 2)

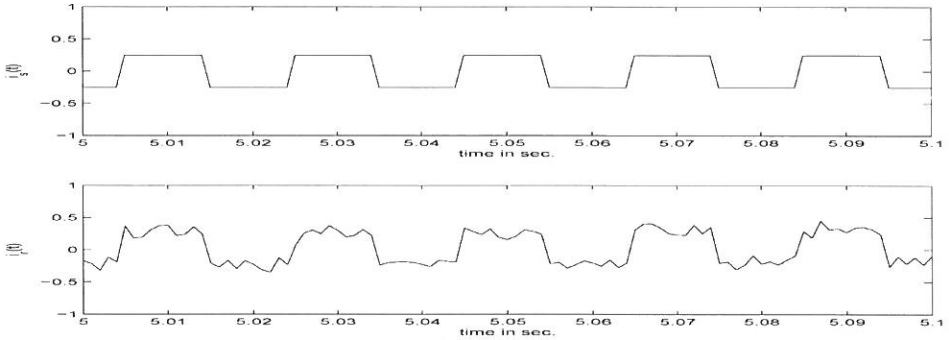

Fig. 26. The plots of $i_s(t)$ and $\bar{i}_s$ versus time using the Sliding Mode controller (m = 2)

CONCLUSION

The synchronization of two hyperchaotic Lü systems is investigated in this paper. Two different cases are studied. The first case is when the number of inputs to the slave system is three. The second case is the more realistic case when the number of inputs to the slave system is two. For each of the cases, two nonlinear control schemes are developed. The first control scheme is a feedback linearization controller. The second control scheme is a sliding mode controller. Both controllers ensure the convergence of the errors between the states of the master and the slave hyperchaotic Lü systems to zero as time tends to infinity.

The simulation results clearly show that the four proposed control schemes are able to synchronize the master and the slave hyperchaotic Lü systems when the two systems start from different initial conditions. It should be noted that sliding mode controllers are generally robust to changes in the parameters of the controlled system. Therefore, sliding mode controllers are usually preferred over feedback linearization controllers.

Furthermore, the proposed control schemes are used for secure communication purposes. The transmitted message is a binary signal consisting of a sequence of zeros and ones. The simulation results indicate that the proposed synchronization controllers are able to recover the transmitted signal even in the presence of zero mean Gaussian noise.

Future research will address the problem of synchronizing other types of hyperchaotic systems as well as synchronizing two different types of hyperchaotic systems.

REFERENCES

Argyris, A. & Syvridis, D. 2010. Chaos Applications in Optical Communications. In Handbook of Information and Communication Security, Springer Berlin Heidelberg, 479-510.

Babtista, M. S. 1998. Cryptography with Chaos. Phys. Letters A, 240, 50-54.

Brandt, M. E. & Chen, G. 1997. Bifurcation control of two nonlinear models of cardiac activity. IEEE Trans. Circ. Syst. I, **44**, 1031-1034.

Chen, A., Lu, J. A., Lu, J. H. & Yu, S. M. 2006. Generating hyperchaotic Lu attractor via state feedback control. Physica A, **364**, 103-110.

Chen, S., Hua, J., Wang, C. & Lu, J. 2004. Adaptive synchronization of uncertain Rossler hyperchaotic system based on parameter identification. Phys. Letters A, **321**, 50-55.

Chen, Z., Yang, Y., Qi, G. & Yuan, Z. 2007. A novel hyperchaos only with one equilibrium. Phys. Letters A, **360 (6)**, 696-701.

Elabbasy, E. M., Agiza, H. N. & El-Dessoky, M. M. 2006. Adaptive synchronization of a hyperchaotic system with uncertain parameter. Chaos, Solitons & Fractals, **30**, 1133-1142.

Feng, J., Chen, S. & Wang, C. 2005. Adaptive synchronization of uncertain hyperchaotic systems based on parameter identification. Chaos, Solitons & Fractals, **26**, 1163-1169.

Gao, B. & Lu, J. 2007. Adaptive synchronization of hyperchaotic Lu system with uncertainty. Chinese Phys. **16**, 0666-0670.

Gao, T., Chen, Z., Yuan, Z. & Yu, D. 2007. Adaptive synchronization of a new hyperchaotic system with uncertain parameters. Chaos, Solitons & Fractals, **33**, 922-928.

Grassi, G. & Mascolo, S. 1999. A system theory approach for designing cryptosystems based on hyperchaos. IEEE Transactions on Circuits and Systems - I:Fundamental Theory and Applications, **46 (9)**, 1135-1138.

Grassi, G. & Miller, D. A. 2002. Theory and experimental realization of observer-based discrete-time hyperchaos synchronization. IEEE Transactions on Circuits and Systems - I: Fundamental Theory and Applications, **49 (3)**, 373-378.

Hsieh, J. Y., Hwang, C. C., Wang, A.P. & Li, W. J. 1999. Controlling hyperchaos of the Rossler system. International J. Control, **72 (10)**, 882-886.

Hu, M., Xu, Z., & Zhang, R. 2008. Full state hybrid projective synchronization in continuous-time chaotic (hyperchaotic) systems. Communications in Nonlinear Science and Numerical Simulations, **13**, 456-464.

Huang, J. 2008. Chaos synchronization between two novel different hyperchaotic systems with unknown parameters. Nonlinear Analysis: Theory, Methods & Applications, **69 (11)**, 4174-4181.

Itoh, M. & Chua, L. O. 2002. Reconstruction And Synchronization Of Hyperchaotic Circuits Via One State Variable," International Journal of Bifurcation and Chaos, **12 (10)**, 2069-2085.

Jang, M., Chen, C. & Chen, C. 2002. Sliding mode control of hyperchaos in Rossler systems. Chaos Solitons & Fractals, **14**, 1465-1476.

Jia, Q. 2007. Adaptive control and synchronization of a new hyperchaotic system with unknown parameters. Phys. Letters A, **362**, 424-429.

Jia, Z., Lu, J. & Deng, G. 2007. Nonlinearly state feedback and adaptive synchronization of hyperchaotic Lu systems. Syst. Eng. Electron. **29**, 598-600.

Jia, N. & Wang, T. 2013. Generation and Modified Projective Synchronization for a Class of New Hyperchaotic Systems. In Abstract and Applied Analysis (Vol. 2013). Hindawi Publishing Corporation.

Kapitaniak, T., Chua, L. O. & Zhong, G-Q. 1994. Experimental hyperchaos in coupled Chua's circuits. IEEE Transactions on Circuits and Systems I: Fundamental Theory and Applications, **41 (7)**, 499-503.

Li, Y., Tang, W. K. S. & Chen, G. R. 2005. Generating hyperchaos via state feedback control. International Journal of Bifurcation Chaos, **15**, 3367-3375.

Lorenz, E. N. 1963. Deterministic non-periodic flows. J. Atmos. Sci. **20**, 130-141.

Matsumoto, T., Chua, L. O. & Kobayashi, K. 1986. Hyperchaos: Laboratory experiment and numerical confirmation. IEEE Trans. Circuits Systems **33(11)**, 1143-1147.

Park, J. H. 2005. Adaptive synchronization of hyperchaotic Chen system with uncertain parameters. Chaos, Solitons & Fractals, **26**, 959-964.

Pecora, L. M. & Caroll, T. L. 1990. Synchronization in chaotic systems. Physical Review Letters, **64(8)**, 821-824

Rafikov, M., & Balthazar, J. M. 2008. On control and synchronization in chaotic and hyperchaotic systems via linear feedback control. Communications in Nonlinear Science and Numerical Simulation, **13(7)**, 1246-1255.

Rossler, O. E. 1979. An equation for hyperchaos. Physics Letters **71A (2-3)**, 155-157.

Sheikhan, M., Shahnazi, R. & Garoucy, S. 2013. Hyperchaos synchronization using PSO-optimized RBF-based controllers to improve security of communication systems. Neural Computing and Applications, 1-12.

Smaoui, N., Karouma, A., & Zribi, M. 2011. Secure communications based on the synchronization of the hyperchaotic Chen and the unified chaotic systems. Communications in Nonlinear Science and Numerical Simulation, **16(8)**, 3279-3293.

Tao, C. & Liu, X. 2007. Feedback and adaptive control and synchronization of a set of chaotic and hyperchaotic systems," Chaos Solitons & Fractals, **32 (14)**, 1572-1583.

Thamilmaran, K., Lakshmanan, M. & Venkatesan, A. 2004. Hyperchaos in a modified canonical Chua's circuit. Int. J. Bifur. & Chaos **14(1)**, 221-243.

Uchida, A. 2012. Generation of Chaos in Lasers. Optical Communication with Chaotic Lasers: Applications of Nonlinear Dynamics and Synchronization, 59-143.

Wang, F. & Liu, C. 2007. Passive control of hyperchaotic Lorenz system and circuit experimental on EWB. International Journal of Modern Phys., B **21**, 3053-3064.

Wu, X., Guan, Z-H. & Wu, Z. 2008. Adaptive synchronization between two different hyperchaotic systems. Nonlinear Analysis: Theory, Methods & Applications, **68(5)**, 1346-1351.

Yan, Z. Y. 2005. Controlling hyperchaos in the new hyperchaotic Chen system. Applied Math. Computers, **168**, 1239-50.

Yassen, M. T. 2008. On hyperchaotic synchronization of a hyperchaotic Lu system. Nonlinear Analysis: Theory, Methods & Applications, **68(11)**, 3592-3600.

Yau, H. T., Hung, T. H. & Hsieh, C. C. 2012. Bluetooth Based Chaos Synchronization Using Particle Swarm Optimization and Its Applications to Image Encryption. Sensors, **12(6)**, 7468-7484.

Zhang, H., Zhao, Y., Yu, W. & Yang, D. 2008. A unifed approach to fuzzy modelling and robust synchronization of different hyperchaotic systems, Chin. Phys. B, **17(2)**, 4056-4066.

Zheng, S., Dong, G. & Bi, Q. 2010. A new hyperchaotic system and its synchronization. Applied Mathematics and Computation, **215(9)**, 3192-3200.

Zhu, C. 2010. Control and synchronize a novel hyperchaotic system. Applied Mathematics and Computation, **216(1)**, 276-284.

Zhu, C. & Sun, K. 2012. Chaos Applications in Digital Watermarking. In Applications of Chaos and Nonlinear Dynamics in Science and Engineering (pp. 187-232). Springer Berlin Heidelberg.

Zribi, M., Hassan, M. F. & Salim, H. 2010. An observer based controller for the synchronization of two Chua's circuits. 10th International Conference in Information Sciences Signal Processing and their Applications (ISSPA), 397-400.

Zribi, M., Oteafy, A. & Smaoui, N. 2009. Controlling chaos in the permanent magnet synchronous motor. Chaos, Solitons & Fractals, **41(3)**, 1266-1276.